Inorganic Chemistry

Article

pubs.acs.org/IC

Structure and Unusual Magnetic Properties of $YbMn_{0.17}Si_{1.88}$

Sebastian C. Peter,[†,‡] Christos D. Malliakas,[⊥] and Mercouri G. Kanatzidis*[,†,§]

[†]Department of Chemistry, Northwestern University, 2145 N. Sheridan Road, Evanston, Illinois 60208-3113, United States

[‡]New Chemistry Unit, Jawaharlal Nehru Centre for Advanced Scientific Research, Jakkur, Bangalore 560064, India

[§]Materials Science Division, Argonne National Laboratory, Argonne, Illinois 60439, United States

[⊥]Department of Chemistry, Northwestern University, 2145 N. Sheridan Road, Evanston, Illinois 60208-3113, United States

Supporting Information

ABSTRACT: $YbMn_{0.17}Si_{1.88}$ was synthesized from the reaction of ytterbium, manganese, and silicon using indium as a flux. The average structure of $YbMn_{0.17}Si_{1.88}$ was refined in the monoclinic space group $P2_1$, with a = 4.0107(8) Å, b = 3.8380(8) Å, c = 14.458(3) Å, β = 97.97(3)°, R1/wR2 = 0.0296/0.0720. The structure can be described as the intergrowth of three AlB_2-type layers and one $BaAl_4$-type layer. Magnetic susceptibility measurements suggest that the ytterbium atoms in $YbMn_xSi_{2-x}$ exist in a mixed valent or intermediate valent state. $YbMn_{0.17}Si_{1.88}$ shows weak antiferromagnetic ordering below ~4.5 K. The magnetic interactions between the Mn and Yb atoms in $YbMn_{0.17}Si_{1.88}$ are evident from the magnetic susceptibility measurements performed at low field. A negative magnetization is observed on warming and a positive magnetization on cooling. The heat capacity data suggest moderate heavy fermion behavior.

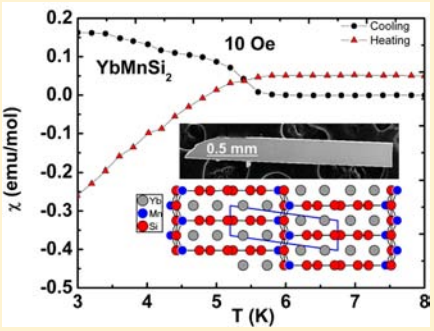

1. INTRODUCTION

In general, rare earth ions in the intermetallic compounds exist in the trivalent state. However, because of the greater stability of the empty, half-filled, or filled 4f shells, the Ce, Eu, and Yb ions may also exist in other valence states, resulting in compounds with unusual physical and magnetic properties. Among them, ytterbium-based compounds are of considerable interest because they can show a wide variety of properties such as Kondo effects in $Yb_2Co_3Ga_9$,[1] heavy fermion behavior in $YbIr_2Si_2$,[2] valence fluctuations in YbCuGa,[3] superconductivity in $YbAlB_4$,[4] etc. These properties are associated with the unstable 4f shell, which can develop two electronic configurations, a completely filled, nonmagnetic divalent (Yb^{2+}) and one electron deficient, magnetic trivalent (Yb^{3+}). A competition between these two states often creates mixed and/or intermediate valent Yb, and this fact is the motivation behind the study of the Yb−Mn−Si system we report here.

The Yb−Mn−Si system has been only briefly studied, and a few of its ternary compounds show unusual physical properties.[5−16] Particularly, $YbMn_2Si_2$[5−9] ($ThCr_2Si_2$ type structure and trivalent Yb) and YbMnSi[10] (TiNiSi type structure and mixed valent Yb) have been studied for their crystal structure and magnetic properties. The pseudoternary compounds of $YbMn_2Si_{2-x}Ge_x$ and $YbMnSi_{1-x}Ge_x$ exhibit valence transitions of the Yb atoms.[10−13] Apart from those systems a brief X-ray powder diffraction study on the $Yb_2Mn_3Si_5$ was reported.[17] The crystal structure of $YbMn_{0.17}Si_{1.83}$ was reported by Norlidah et al.[16] crystallizing in the orthorhombic system with lattice constants a = 4.0191(5) Å, b = 28.649(4) Å, c = 3.8418(5) Å. However, the unrealistic bond distances (Mn−Si (1.880(6) Å)) and huge thermal parameters for the silicon atoms in the structure raised doubts about the accuracy of the crystal structure. Norlidah et al. used the propagation vector [0, 0, $^1/_3$] for the Si atoms and [$^1/_3$, 0, $^1/_3$] for the Mn atoms to remove these problems.

Following our previous investigation of anomalous thermal expansion in the square net $Yb_4T_xGe_8$ (T = Cr−Ni, Ag) compounds[18] and considering the fact that only $YbNiSi_2$ in the $CeNiSi_2$ type structure[19] has been reported, we focused our studies on the synthesis of Mn analogues via reactions in liquid indium. These reactions led to single crystals of $YbMn_{0.17}Si_{1.88}$, the structure of which was refined using X-ray single crystal data. $YbMn_{0.17}Si_{1.88}$ crystallizes in the rare monoclinic polar space group $P2_1$, which is an ordered structure of the compound reported by Norlidah et al.[16] Magnetic susceptibility studies on selected single crystals of $YbMn_{0.17}Si_{1.88}$ show that it is an intermediate/mixed Yb valent compound exhibiting a magnetic transition associated with valence change. This unusual magnetic behavior is also reflected in the specific heat measurements.

2. EXPERIMENTAL SECTION

Reagents. The following reagents were used: Yb (in the form of powder ground from metal chunk, 99.9%, Chinese Rare Earth Information Center, Inner Mongolia, China), Mn (powder, 99.9% Aldrich Chemical Co., Inc.), Si (pieces, 99.999%, Dow Corning), and In (drops, 99.999% Cerac Inc., Milwaukee, WI).

Synthesis. Single crystals of $YbMn_{0.17}Si_{1.88}$ were obtained by combining 3 mmol of ytterbium, 2 mmol of manganese, 6 mmol of silicon, and 45 mmol of indium in an alumina crucible under an inert

Received: November 15, 2012
Published: April 25, 2013

   dx.doi.org/10.1021/ic3024925 | Inorg. Chem. 2013, 52, 4909−4915

nitrogen atmosphere inside a glovebox. The crucible was placed in a 13 mm fused silica tube, which was flame-sealed under vacuum of 10^{-4} Torr, to prevent oxidation during heating. The reactants were then heated to 1000 °C over 10 h, maintained at that temperature for 5 h to allow proper homogenization, followed by cooling to 850 °C in 2 h, and held there for 48 h. Finally, the system was allowed to slowly cool to 50 °C in 48 h. The reaction product was isolated from the excess indium flux by heating at 350 °C and subsequent centrifugation through a coarse frit. Any remaining flux was removed by immersion and sonication in glacial acetic acid for 48 h. The final crystalline product was rinsed with water and dried with acetone. Several crystals, which grow as metallic silver rods, were carefully selected for elemental analysis, structure characterization, and the physical property measurements. The main product obtained from the reaction is $YbMn_{0.17}Si_{1.88}$ along with a secondary binary phase Mn_3Si.

Synthesis of $YbMn_{0.17}Si_{1.88}$ using conventional synthesis techniques such as direct heating in a regular furnace and high frequency induction furnace was not successful in producing single phase of $YbMn_{0.17}Si_{1.88}$. Attempts to synthesize single phase compound using Ga and Sn fluxes also were not successful.

Elemental Analysis. Quantitative microprobe analyses of the compound were performed with a Hitachi S-3500 scanning electron microscope (SEM) equipped with a PGT energy dispersive X-ray analyzer. Data were acquired with an accelerating voltage of 20 kV and a 60 s accumulation time. Energy dispersive spectroscopy (EDS) performed on visibly clean surfaces of the samples gave the atomic composition is in good agreement with the results derived from the single crystal X-ray diffraction refinement. The EDS composition is $Yb_{1.00(6)}Mn_{0.17(2)}Si_{1.88(9)}$, averaged over 5 different crystals. The error is given as the standard deviation on the obtained composition for the individual crystals.

X-ray Crystallography. The X-ray intensity data on selected single crystals of $YbMn_{0.17}Si_{1.88}$ were collected at 100 K using a STOE IPDS 2T diffractometer with graphite-monochromatized Mo Kα (λ = 0.710 73 Å) radiation. The X-AREA (X-RED and X-SHAPE within) package suite[20] was used for the data extraction and integration to apply empirical and analytical absorption corrections. The structure of the compound was solved by direct methods and refined using SHELXL-97 (full-matrix least-squares on F^2)[21] with anisotropic atomic displacement parameters for all atoms.

Structure Refinement. Indexing of first few frames obtained from the diffractometer led to a C-centered orthorhombic cell. Similar to the work reported by Norlidah et al., the structure was refined initially in the orthorhombic space group *Cmcm*, and a total of seven atomic positions were identified. The site occupancy of Mn was reduced to 32%, Si4 was reduced to 78%, and other sites were found to be fully occupied. In this model many bond distances were too short to make chemical sense; for example, Mn−Si3 distance is 1.87 Å (Mn−Si covalent bond length is 2.54 Å). In addition to these short distances, the anisotropic displacements of Si3 and Si4 were enlarged along the *c* axis (U_{33} for Si3 > 56 × 10^3 Å^2 and U_{33} for Si4 > 149 × 10^3 Å^2). The mixed occupancy, unusual thermal displacement parameters, and unphysical distances are an artifact of a superstructure in $YbMn_{0.17}Si_{1.88}$. This is reminiscent of the structure of $YbSi_{1.4}$ which exhibits both commensurate and incommensurate modulated structures determined by high-resolution transmission electron microscopy (HRTEM) studies.[22] In the case of $YbSi_{1.4}$ the basic substructure was also initially refined in the orthorhombic cell with space group *Cmcm*, and the lattice constants are a = 4.159(1) Å, b = 23.510(5) Å, c = 3.775(1) Å. However, the previous HRTEM studies on $YbSi_{1.4}$ showed two distinct ordering variants: the first one having a doubled unite cell volume, orthorhombic *Imm*2 space group, and lattice constants are a = 4.16 Å, b = 7.56 Å, c = 23.51 Å, while the second one has an incommensurate 3 + 1-dimensional superspace group *Cmcm*(10γ). Our recent work on RET_xGe_2 (RE = Gd, Yb; T = Cr−Ni, Ag),[18] also showed the partial occupation of transition metal created an unacceptable structural refinement and was successfully refined using a (3 + 1)D crystallographic approach. All these works motivated us to check for supercell reflections observed in the reciprocal space due to the modulation of the Si atom in the extended square net. Our preliminary refinement showed that $YbMn_{0.17}Si_{1.88}$ adopts *Pm*(\a1/2\g)*s* space group and lattice constants are a = 4.011(8) Å, b = 3.8389(8) Å, c = 14.4516(3) Å, β = 97.958(3)°. The **q**-vector for the compound is commensurate and along the *c*-axis in the form of 1/4c*. However, relatively large residual (R_1 > 6%) and relatively huge anisotropic displacement parameters (U_{22} of Si5 > 135 Å^2 × 10^3) made this model unlikely as the correct refinement.

Another possibility is to reduce the symmetry and refine the crystal structure in a lower symmetry space group. For this purpose we have reduced the symmetry and indexed the lattice constants in the monoclinic system. The crystal structure of $YbMn_{0.17}Si_{1.88}$ could be refined in the space group $P2_1$ with lattice constants a = 4.0107(8) Å, b = 3.8380(8) Å, c = 14.458(3) Å β = 97.958(3)°. The relatively large displacement parameters of the Si3 and Si4 atoms imply that distortions are present in these positions. The structure was solved by direct methods and refined using SHELXL-97 (full-matrix least-squares on F^2)[21] with anisotropic atomic displacement parameters for all atoms. As a check for the correct composition, the occupancy parameters were refined in a separate series of least-squares cycles. A total of seven atomic positions were identified. The site occupancy of Mn was reduced to 33% and of Si4 to 77% while all other sites were found to be fully occupied. Data collection and refinement details are given in Table 1. The final atomic positions and equivalent isotropic displacement parameters are given in Table 2 and anisotropic displacement parameters in Table 3. The selected bond distances are listed in Table 4. It is noteworthy to further comment on the thermal displacement parameters of Si3 and Si4 which are abnormally large, and that of Yb2 (U11) which is rather small. We have reported such behavior previously in layered systems with square nets of main group atoms.[18] It is a consequence of local displacements (often in-plane) which may or may not be commensurate or coherent with respect to the underlying lattice. When they are commensurate a superstructure or modulation with **q**-vectors is observed. In our case these distortions do not appear to be coherent and could not be observed in the diffraction data. One way to tackle this issue and probe

Table 1. Crystal Data and Structure Refinement for $YbMn_{0.17}Si_{1.88}$ at 293(2) K[a]

wavelength	0.710 73 Å
cryst syst	monoclinic
space group	$P2_1$
unit cell dimensions	a = 4.0107(8) Å, α = 90.00°
	b = 3.8380(8) Å, β = 97.97(3)°
	c = 14.458(3) Å, γ = 90.00°
V	220.40(8) Å^3
Z	1
density (calcd)	7.088 g/cm^3
abs coeff	43.902 mm^{-1}
F(000)	402
cryst size	0.10 × 0.08 × 0.08 mm^3
θ range for data collection	2.85° to 29.10°
index ranges	$-5 \le h \le 5$, $-5 \le k \le 5$, $-19 \le l \le 19$
reflns collected	2115
indep reflns	1188 [R_{int} = 0.0408]
completeness to θ = 29.10°	99.3%
refinement method	full-matrix least-squares on F^2
data/restraints/params	1188/1/68
GOF	1.143
final R indices [>2σ(I)]	R_{obs} = 0.0296, wR_{obs} = 0.0720
R indices [all data]	R_{all} = 0.0337, wR_{all} = 0.0742
extinction coeff	0.0047(7)
largest diff peak and hole	2.320 and −3.053 e Å^{-3}

[a] $R = \Sigma||F_o| - |F_c||/\Sigma|F_o|$, wR = $\{\Sigma[w(|F_o|^2 - |F_c|^2)^2]/\Sigma[w(|F_o|^4)]\}^{1/2}$, and calcd $w = 1/[\sigma^2(F_o^2) + (0.0449P)^2 + 1.3738P]$ where $P = (F_o^2 + 2F_c^2)/3$.

dx.doi.org/10.1021/ic3024925 | Inorg. Chem. 2013, 52, 4909−4915

Table 2. Atomic Coordinates (×10^4) and Equivalent Isotropic Displacement Parameters (Å^2 × 10^3) for $YbMn_{0.17}Si_{1.88}$ at 293(2) K with Estimated Standard Deviations in Parentheses

label	x	y	z	occupancy	U_{eq}[a]
Yb(1)	9404(1)	4508(3)	8806(1)	1	2(1)
Yb(2)	8289(1)	9512(2)	6578(1)	1	2(1)
Mn(1)	2755(11)	4610(40)	5536(3)	0.337(8)	3(2)
Si(1)	3572(6)	4540(20)	7140(2)	1	6(1)
Si(2)	5941(6)	4590(20)	1872(2)	1	6(1)
Si(3)	2510(12)	9520(40)	5017(2)	1	33(2)
Si(4)	5127(11)	5236(15)	265(4)	0.777(19)	18(2)

[a] U_{eq} is defined as one-third of the trace of the orthogonalized U_{ij} tensor.

Table 3. Anisotropic Displacement Parameters (Å^2 × 10^3) for $YbMn_{0.17}Si_{1.88}$ at 293(2) K with Estimated Standard Deviations in Parentheses[a]

label	U_{11}	U_{22}	U_{33}	U_{12}	U_{13}	U_{23}
Yb(1)	1(1)	2(1)	3(1)	0	0	0
Yb(2)	4(1)[b]	1(1)	6(1)	0(2)	0	0
Mn(1)	4(2)	1(2)	3(2)	1(1)	0(2)	0(1)
Si(1)	2(1)	3(1)	11(2)	1(1)	0	0
Si(2)	2(1)	2(2)	15(2)	0(1)	0(1)	0(1)
Si(3)	37(2)	59(3)	4(2)	1(1)	0	1(1)
Si(4)	4(2)	34(5)	8(2)	0(1)	0(1)	0(1)

[a] The anisotropic displacement factor exponent takes the form $-2\pi^2[h^2a^{*2}U_{11} + ... + 2hka^*b^*U_{12}]$. [b] Multiplied by 10^4.

Table 4. Bond Lengths [Å] for $YbMn_{0.17}Si_{1.88}$ at 293(2) K with Estimated Standard Deviations in Parentheses

label	distance	label	distance
Yb(1)−Si(1)	3.116(3)	Yb(2)−Si(3)	2.985(10)
Yb(1)−Si(1)	3.117(3)	Yb(2)−Si(3)	3.002(4)
Yb(1)−Si(2)	2.917(5)	Yb(2)−Mn(1)	3.028(5)
Yb(1)−Si(2)	2.921(5)	Yb(2)−Mn(1)	3.125(10)
Yb(1)−Si(2)	2.961(7)	Mn(1)−Si(1)	2.296(5)
Yb(1)−Si(2)	2.964(7)	Mn(1)−Si(3)	2.03(2)
Yb(1)−Si(4)	2.908(5)	Mn(1)−Si(3)	2.09(2)
Yb(1)−Si(4)	2.910(5)	Mn(1)−Si(3)	2.152(6)
Yb(1)−Si(4)	2.913(5)	Mn(1)−Si(3)	2.161(6)
Yb(1)−Si(4)	3.258(5)	Mn(1)−Mn(1)	3.165(7)
Yb(1)−Si(4)	3.261(6)	Si(2)−Si(1)	2.368(10)
Yb(2)−Si(1)	2.881(6)	Si(2)−Si(1)	2.399(9)
Yb(2)−Si(1)	2.899(6)	Si(3)−Si(3)	2.775(7)
Yb(2)−Si(2)	2.989(3)	Si(4)−Si(4)	2.064(4)
Yb(2)−Si(2)	2.992(3)	Si(4)−Si(2)	2.314(6)
Yb(2)−Si(3)	2.981(9)		

these distortions is to perform pair distribution function analysis which takes into account the diffuse scattering caused by the nonperiodic distortions.[23,24] This is a separate study and outside the scope of this paper.

Magnetic Measurements. Magnetic susceptibility measurements were carried out with a Quantum Design MPMS SQUID magnetometer. The selected single crystals of $YbMn_{0.17}Si_{1.88}$ were used for the magnetic measurements. Temperature dependent data were collected for both zero field cooled (ZFC) and field cooled mode (FC) between 2 and 300 K, with applied field from 1 to 50 kG. A typical measurement consists of initial cooling from room temperature (300 K) down to 2 K with no applied field, and then the selected field is turned on and the ZFC data are collected on warming, followed by cooling back to 2 K and collect FC data on warming with the applied field still on. In order to check the complex and unusual magnetic behavior at low temperature, the magnetic data were collected during both cooling and warming process. Field dependent magnetic measurements were acquired at 2, 5, 10, 15, and 20 K with field sweeping from −50 up to 50 kG.

Specific Heat. Heat capacity (C) measurements were performed on selected single crystals of $YbMn_{0.17}Si_x$ by relaxation method using QD-PPMS. The sample was glued to calibrated HC-puck using Apizeon N grease. C was measured in the 3−20 K range with no applied magnetic fields (H).

3. RESULTS AND DISCUSSION

3.1. Reaction Chemistry. The metal flux technique has been used widely for the crystal growth of binary or ternary phases both as reactive and nonreactive solvents.[18,25−47] Carrying out reactions between Yb, T, and Si in liquid indium favors the formation of YbT_2Si_2[11] as the main compound and a few single crystals of AlB_2-type $YbSi_2$ as a side product. Our recent investigations in the Yb/T/Si system in indium flux produced the compounds YbT_xSi_{2-x} (T = Cr, Fe, Co) which crystallize in the $ThSi_2$ structure type.[42] However, no Mn analogues were obtained under the same reaction conditions. Only when an excess of Mn was used did we obtain plate shaped gray crystals of $YbMn_{0.17}Si_{1.88}$. Powder XRD confirmed that this phase did not crystallize in the $ThSi_2$ structure type. Mn_3Si was the main impurity observed in this reaction in addition to some unreacted silicon. $YbMn_{0.17}Si_{1.88}$ single crystals have metallic luster and are stable in air for months. In order to suppress the main impurity of Mn_3Si attempts were made using Sn and Ga as fluxes. Neither of these alternative fluxes succeeded in producing the corresponding YbT_xSi_{2-x} compounds. A typical scanning electron micrograph of a $YbMn_{0.17}Si_{1.88}$ single crystal is shown in the Supporting Information (Figure S1).

3.2. Crystal Structure. $YbMn_{0.17}Si_{1.88}$ crystallizes in the monoclinic system. The average structure is shown in Figure 1B, and is closely related to the previously reported disordered orthorhombic structure (Figure 1A). The structure can be described as the stacking of three AlB_2 and one $BaAl_4$ slabs along the [010] direction with the Yb atoms residing within the channels formed by the connection of the two layers. Alternatively, the structure can also be described as Mn and Si atoms (excluding Yb atoms) located in alternating layers stacked along the long *c*-axis in the following sequence: Mn−Si1−Si2−Si4−Si4−Si2−Si1−Mn. The bonds to the Yb atoms are omitted in the figure to emphasize the three-dimensional (3D) Mn/Si framework and its channels. The $BaAl_4$ slab is formed by partially filled manganese sites and fully occupied Si3 sites, while the AlB_2 slabs are formed by ytterbium and three Si atoms. Mn and Si3 atoms in the $BaAl_4$ slab are arranged as distorted square nets (Figure 1C). In this, the tetrahedrally coordinated (4 Mn atoms) Si3 atoms form a 2-dimensional square net that extends in the *ac*-plane and is capped by Mn atoms alternatively above and below this plane forming an overall puckered layer. The AlB_2 layers on the other hand are composed of two different types of Si zigzag chains (Figure 1D). The layer containing Si4 atoms is less puckered (Si4−Si4−Si4 bond angle is 136.7°) compared to the layer containing Si2 and Si1 atoms (Si2−Si1−Si2 bond angle is 107.2°). These layers are connected along the *c*-axis forming Si_6 hexagons and connected in a slightly distorted fashion (Figure 2) adopting an overall monoclinic system.

dx.doi.org/10.1021/ic3024925 | Inorg. Chem. 2013, 52, 4909−4915

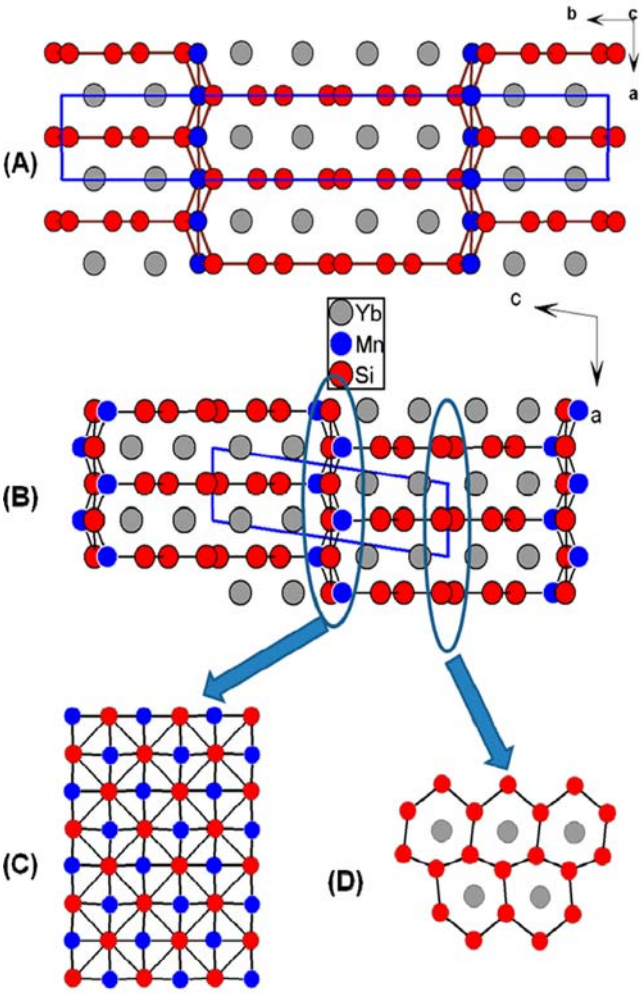

Figure 1. (A) Crystal structure of $YbMn_{0.17}Si_{1.88}$ in the orthorhombic system projected along [001]. (B) Crystal structure of $YbMn_{0.17}Si_{1.88}$ in the monoclinic system projected along [010]. (C) $BaAl_4$ type layer. (D) AlB_2 layer.

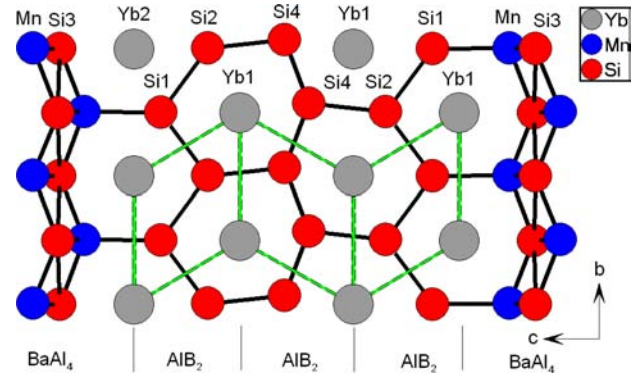

Figure 2. $BaAl_4$ and AlB_2 slabs in the crystal structure of $YbMn_{0.17}Si_{1.88}$. The unit cell of three AlB_2 layers are marked with solid green lines.

Structural refinement in the monoclinic system improved the bond distances compared to the refinement in the previously reported orthorhombic system.[16] The shortest Si−Si distance 2.0467 Å is much shorter than the typical Si−Si covalent bond length of 2.34 Å, but such short distances have reported in $Yb_2Fe_4Si_9$ (2.07 Å)[48] and in the Zintl phase $CaSi_2$ (2.11 Å) at 360 kbar.[49] The 3d electrons of Mn and 4f electrons likely contribute to the Mn−Yb2 bond, and this electron transfer seems to create the mixed valence at the Yb sites ($Yb^{(2+\delta)}$). As a result the Mn−Si2 distances are very short (2.0298 Å) in the square net.

The coordination environments of the two Yb atoms are shown in Figure 3. Both sites have high coordination number

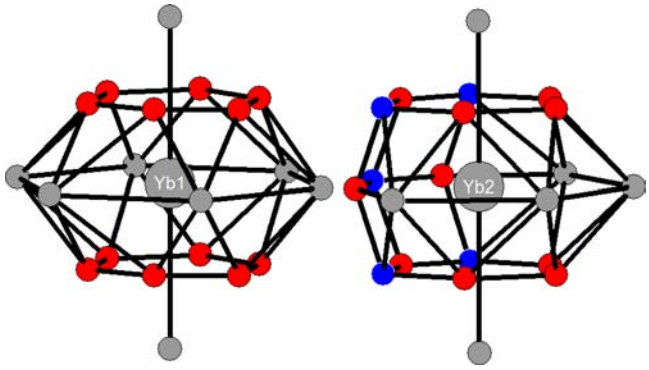

Figure 3. Cagelike nearest neighbor environments of the two Yb positions in $YbMn_{0.17}Si_{1.88}$.

(CN) as is usual for such intermetallic compounds: CN 20 for Yb1 with 12 Si + 8 Yb for Yb1 and CN 21 for Yb2 with 10 Si + 5 Mn + 6 Yb for Yb2. Although the coordination numbers of both ytterbium sites are similar, there are negligible differences in the interatomic distances. The 12 nearest silicon neighbors of Yb1 site has Yb−Si distances ranging from 2.91 to 3.25 Å and Yb2 has closest Si neighbors within the range 2.88−3.01 Å. These contacts are most likely bonding. It is also interesting to mention Yb2 has no closest Mn atom compared to 5 Mn atoms in the case of Yb1. The average Yb−Si and Yb−Yb distances for Yb1 and Yb2 are 2.983 and 3.873 Å, and 2.951 and 3.857 Å, respectively. These suggest no significant differences between ytterbium sites. The average Yb−Mn distance obtained for Yb2 is 3.126 Å, which is longer than the average Yb−Si distance and consistent with the larger size of Mn atom compared to Si.

3.3. Magnetism. The temperature dependent magnetic susceptibility of $YbMn_{0.17}Si_{1.88}$ at an applied field of 1 kOe and the inverse molar magnetic susceptibility $1/\chi_m(T)$ data versus the temperature are shown in Figures 4 and 5, respectively. Above 40 K $YbMn_{0.17}Si_{1.88}$ exhibits paramagnetic behavior following Curie−Weiss law $\chi_m(T) = C/(T - \theta_p)$,[50] where $C = N_A\mu_{eff}^2/3k_B = \mu_{eff}^2/8$ is the Curie constant and θ_p is the Weiss temperature. Linear least-squares fit of the data to this equation within the linear region 50−200 K gives an effective moment μ_{eff} of 3.32 μ_B per formula and θ_p of −136 K. In general, the

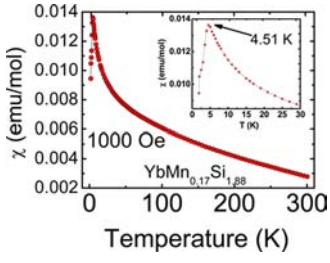

Figure 4. Magnetic susceptibility ($\chi = M/H$) as a function of temperature for $YbMn_{0.17}Si_{1.88}$ (polycrystalline) sample measured in a dc field of 1 kOe. The inset figure shows magnetic ordering at ~5 K.

dx.doi.org/10.1021/ic3024925 | Inorg. Chem. 2013, 52, 4909−4915

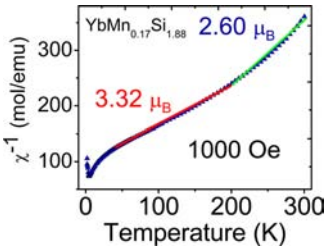

Figure 5. Inverse magnetic susceptibility (χ^{-1} = H/M) for polycrystalline sample of $YbMn_{0.17}Si_{1.88}$. The linear regions are marked with red and green solid lines.

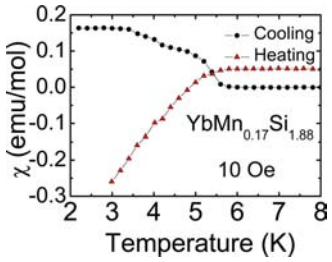

Figure 6. Temperature dependent susceptibility for $YbMn_{0.17}Si_{1.88}$ obtained on cooling and warming under 10 Oe.

negative θ_p corresponds to predominant antiferromagnetic interactions in the compound. Above 200 K a slight deviation from linearity is observed, and the calculated magnetic moment in the range 200−300 K is ∼2.60 μ_B/Yb (57% of Yb^{3+}), which may be indicating a valence change occurring at ∼200 K. A detailed temperature dependent X-ray absorption near edge spectroscopy is required to further confirm this speculation. Below 40 K the $\chi_m(T)$ data do not obey CW law, and below 4.51 K the compound orders antiferromagnetically.

Field dependent magnetic susceptibility measurements performed on $YbMn_{0.17}Si_{1.88}$ within the temperature range 2−300 K are shown in the Supporting Information, Figure S2. At low applied magnetic field 10 and 50 Oe, a sudden negative magnetization was observed at 4.5 K, which we initially speculated to be a superconducting transition either from the compound or from adventitious indium in the samples. In order to check this possibility the susceptibility measurement were performed on In metal with the same conditions, and the comparison is shown in the Supporting Information, Figure S3. Indium is superconducting at 3.5 K,[51] and this is reflected in the magnetic susceptibility measurements at lowest field possible (10 Oe). This difference clearly confirms that the negative magnetization of $YbMn_{0.17}Si_{1.88}$ is not from adventitious indium but from the compound. Electrical resistivity measurements (shown in the Supporting Information Figure S4) show that there is no drop in resistivity around 4.5 K. Instead at 3 K the resistivity drop about 3% indicating traces of indium flux in the crystals of $YbMn_{0.17}Si_{1.88}$.

Recently, Andrzejewski et al. explained[52] a similar negative magnetization of $YbFe_4Al_8$ which was previously described as an antiferromagnetic superconductor.[53] On the basis of detailed studies, they ruled out the existence of superconductivity and proposed a mechanism in terms of antiferromagnetic interactions between the moment of Yb and the effective moment of canted Fe spins. Considering a similar explanation for $YbMn_{0.17}Si_{1.88}$, magnetic susceptibility measurements were performed at the smallest possible applied magnetic field of 10 Oe on cooling and on warming, Figure 6. During cooling (black circles) the magnetic susceptibility increased in good agreement with Curie−Weiss law. The second line (red triangles) represents the data upon warming. The cooling and warming curves bifurcate at 5.8 K and the negative magnetization is observed in the warming data. A similar trend in magnetic behavior was observed for some manganese based perovskites like $Gd_{0.67}Ca_{0.33}MnO_3$,[54] $La_{1-x}Gd_xMnO_3$,[55] and $TbMnO_3$[56] although the origin of magnetism in perovskites and in $YbMn_{0.17}Si_{1.88}$ may be different. Here, we adapted the model proposed by Cooke et al.[57] which was used for the interpretation of negative magnetization of $YbFe_4Al_8$.[52] According to this model, at around the magnetic ordering temperature of $YbMn_{0.17}Si_{1.88}$, a spontaneous ferromagnetic moment forms due to the canting of Mn spins. The paramagnetic moment of Yb is induced by both the applied magnetic field and canted Mn spins. When the paramagnetic moment of Yb dominates over the unaffected by temperature ferromagnetic manganese, the system may exhibit a negative magnetization. However, a detailed neutron diffraction study and magnetic structure calculations will be required to investigate these hypotheses.

Magnetization measurements of $YbMn_{0.17}Si_{1.88}$ carried at various temperatures starting from 2 K is shown in the Supporting Information, Figure S5. As the temperature is raised to well above the ordering temperature (10 K) a smooth curve is obtained over the complete range of applied field which continues to higher temperatures.

3.4. Specific Heat. Figure 7 shows the specific heat of $YbMn_{0.17}Si_{1.88}$ within the temperature range 2−50 K with zero

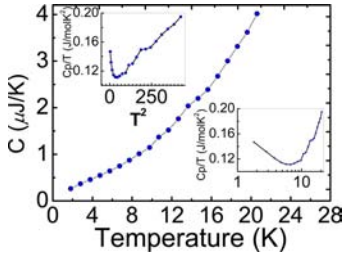

Figure 7. Heat capacity C_p for $YbMn_{0.17}Si_{1.88}$ measured as a function of temperature (T) at zero applied field. The inset figures show C_p/T vs T and C_p/T vs T^2.

applied field. The inset figures shown are (a) C/T versus T and (b) C/T versus T^2. Within the Debye low temperature approximation the measured specific heat is given as

$$C = \gamma T + \beta T^3 \text{ or } C/T = \gamma + \beta T^2 \quad (1)$$

where γ is the contribution from the conduction electrons and β is the lattice contribution.[58] The value of γ is proportional to the density of states near the Fermi energy. A fit to the experimental points resulted in a Debye temperature Θ_D of about 115 K, and an electronic specific heat coefficient $\gamma \approx 170$ mJ/mol K^2, which was determined from γ (=C_p vs $T)_{T\to 0}$ at low temperatures. Therefore, the compound may be a moderate heavy-fermion material according to the arbitrary classification of these systems into "light", "moderate", and classical heavy-fermions with γ values lying in the ranges ∼50−100, 100−400, and >400 mJ/mol K^2, respectively.

Temperature dependent specific heat shows a smooth curve from 2 to 300 K, but both (a) C/T versus T and (b) C/T versus T^2 show anomalies (10 and 13 K in C/T vs T) which

dx.doi.org/10.1021/ic3024925 | Inorg. Chem. 2013, 52, 4909−4915

highlight the magnetic instabilities in this compound. The upturn in (a) C/T versus T and (b) C/T versus T^2 observed at low temperatures is characteristic of many heavy fermion and moderate heavy fermion compounds.[59] In order to study the influence of the magnetic field on the specific heat further, field dependent measurements will be needed. The semilog plot in the inset of Figure 7 emphasizes the logarithmic increase of the electronic specific heat coefficient below 6 K in zero magnetic field. This type of dependence in the low-temperature part of $C(T)/T$ plot is reminiscent of non-Fermi-liquid (NFL) behavior,[60] which may be from the presence of the magnetic phase transition at low temperature.

4. CONCLUDING REMARKS

$YbMn_{0.17}Si_{1.88}$ crystallizes in the polar noncentrosymmetric space group $P2_1$. The compound orders antoiferromagnetically at 4.51 K, and the magnetic properties are consistent with a valence change occurring in the structure. An unusual negative magnetization is observed in $YbMn_{0.17}Si_{1.88}$ at ∼5.8 K which may be explained using the model proposed by Cooke et al.[57] This interaction is prominent at lower field, which makes the total moment of $YbMn_{0.17}Si_{1.88}$ negative. The influence of Mn spins on the total magnetism is evident from the field dependent magnetic susceptibility, magnetization, and specific heat studies. The magnetic structure of this compound should further be studied with neutron diffraction and magnetic structure calculations.

■ ASSOCIATED CONTENT

Supporting Information

Crystallographic data in CIF format. Additional figures. This material is available free of charge via the Internet at http://pubs.acs.org.

■ AUTHOR INFORMATION

Corresponding Author

*E-mail: m-kanatzidis@northwestern.edu (M.G.K.). Phone: 847-467-1541. Fax: 847-491-5937.

Notes

The authors declare no competing financial interest.

■ ACKNOWLEDGMENTS

Work at Argonne National Laboratory is supported by UChicago Argonne, a U.S. DOE Office of Science Laboratory, operated under Contract DE-AC02-06CH11357.

■ REFERENCES

(1) Dhar, S. K.; Mitra, C.; Manfrinetti, P.; Palenzona, A.; Bonville, P. *Physica B* **1999**, *261*, 150.
(2) Danzenbacher, S.; Kucherenko, Y.; Laubschat, C.; Vyalikh, D. V.; Hossain, Z.; Geibel, C.; Zhou, X. J.; Yang, W. L.; Mannella, N.; Hussain, Z.; Shen, Z. X.; Molodtsov, S. L. *Phys. Rev. Lett.* **2006**, *96*, 106402.
(3) Adroja, D. T.; Malik, S. K.; Padalia, B. D.; Bhatia, S. N.; Walia, R. *Phys. Rev. B* **1990**, *42*, 2700.
(4) Nakatsuji, S.; Kuga, K.; Machida, Y.; Tayama, T.; Sakakibara, T.; Karaki, Y.; Ishimoto, H.; Yonezawa, S.; Maeno, Y.; Pearson, E.; Lonzarich, G. G.; Balicas, L.; Lee, H.; Fisk, Z. *Nat. Phys.* **2008**, *4*, 603.
(5) Okada, S.; Kudou, K.; Mori, T.; Iizumi, K.; Shishido, T.; Tanaka, T.; Rogl, P. *J. Cryst. Growth* **2002**, *244*, 267.
(6) Szytula, A.; Jezierski, A.; Penc, B.; Hofmann, M.; Campbell, S. J. *J. Alloys Compd.* **2004**, *363*, 46.
(7) Rossi, D.; Marazza, R.; Mazzone, D.; Ferro, R. *J. Less-Common Met.* **1978**, *59*, 79.
(8) Hofmann, M.; Campbell, S. J.; Edge, A. V. J.; Studer, A. J. *J. Phys.: Condens. Matter* **2001**, *13*, 9773.
(9) Szytula, A.; Szott, I. *Solid State Commun.* **1981**, *40*, 199.
(10) Fornasini, M. L.; Merlo, F.; Palenzona, A.; Pani, M. *J. Alloys Compd.* **2002**, *335*, 120.
(11) Nowik, I.; Felner, I.; Bauminger, E. R. *J. Magn. Magn. Mater.* **1998**, *185*, 91.
(12) Ryan, D. H.; Cadogan, J. M.; Edge, A. V. J. *J. Phys.: Condens. Matter* **2004**, *16*, 6129.
(13) Hofmann, M.; Campbell, S. J.; Edge, A. V. J. *J. Magn. Magn. Mater.* **2004**, *272*, E489.
(14) Ferro, R.; Saccone, A.; Delfino, S.; Maccio, D.; Giovannini, M. *Powder Metall. Metal Ceram.* **1997**, *36*, 117.
(15) Ryan, D. H.; Cadogan, J. M. *Hyperfine Interact.* **2004**, *153*, 43.
(16) Norlidah, N. M.; Ijjaali, I.; Venturini, G.; Malaman, B. *J. Alloys Compd.* **1998**, *278*, 246.
(17) Meotmeyer, M.; Venturini, G.; Malaman, B.; Mcrae, E.; Roques, B. *Mater. Res. Bull.* **1985**, *20*, 1009.
(18) Peter, S. C.; Chondroudi, M.; Malliakas, C. D.; Balasubramanian, M.; Kanatzidis, M. G. *J. Am. Chem. Soc.* **2011**, *133*, 13840.
(19) Bodak, O. I.; Gladyshevskii, E. I. *Sov. Phys. Crystallogr. USSR* **1970**, *14*, 859.
(20) *X-AREA, I.S.*; STOE & Cie GmbH: Darmstadt, 2006.
(21) *SHELXTL, S.10 ed.*; Bruker Analytical X-ray Systems, Inc.: Madison, WI, 1998.
(22) Kubata, C.; Krumeich, F.; Worle, M.; Nesper, R. *Z. Anorg. Allg. Chem.* **2005**, *631*, 546.
(23) Bud'ko, S. l.; Islam, Z.; Wiener, T. A.; Fisher, I. R.; Lacerda, A. H.; Canfield, P. C. *J. Magn. Magn. Mater.* **1999**, *205*, 53.
(24) Canfield, P. C.; Fisk, Z. *Philos. Mag. B* **1992**, *65*, 1117.
(25) Chondroudi, M.; Peter, S. C.; Malliakas, C. D.; Balasubramanian, M.; Li, Q. A.; Kanatzidis, M. G. *Inorg. Chem.* **2011**, *50*, 1184.
(26) Fisher, I. R.; Islam, Z.; Canfield, P. C. *J. Magn. Magn. Mater.* **1999**, *202*, 1.
(27) Hundley, M. F.; Sarrao, J. L.; Thompson, J. D.; Movshovich, R.; Jaime, M.; Petrovic, C.; Fisk, a. Z. *Phys. Rev. B* **2001**, *65*, 024401.
(28) Kanatzidis, M. G.; Pottgen, R.; Jeitschko, W. *Angew. Chem., Int. Ed.* **2005**, *44*, 6996.
(29) Macaluso, R. T.; Sarrao, J. L.; Moreno, N. O.; Pagliuso, P. G.; Thompson, J. D.; Fronczek, F. R.; Hundley, M. F.; Malinowski, A.; Chan, J. Y. *Chem. Mater.* **2003**, *15*, 1394.
(30) Nicklas, M.; Sidorov, V. A.; Borges, H. A.; Pagliuso, P. G.; Petrovic, C.; Fisk, Z.; Sarrao, J. L.; Thompson, J. D. *Phys. Rev. B* **2004**, *67*, 020506.
(31) Peter, S. C.; Kanatzidis, M. G. *Z. Anorg. Allg. Chem.* **2012**, *638*, 287.
(32) Peter, S. C.; Malliakas, C. D.; Nakkotte, H.; Kothapilli, K.; Rayaprol, S.; Schultz, A. J.; Kanatzidis, M. G. *J. Solid. State Chem.* **2012**, *187*, 200.
(33) Peter, S. C.; Rayaprol, S.; Francisco, M. C.; Kanatzidis, M. G. *Eur. J. Inorg. Chem.* **2011**, 3963.
(34) Salvador, J. R.; Bilc, D.; Gour, J. R.; Mahanti, S. D.; Kanatzidis, M. G. *Inorg. Chem.* **2005**, *44*, 8670.
(35) Salvador, J. R.; Gour, J. R.; Bilc, D.; Mahanti, S. D.; Kanatzidis, M. G. *Inorg. Chem.* **2004**, *43*, 1403.
(36) Salvador, J. R.; Hoang, K.; Mahanti, S. D.; Kanatzidis, M. G. *Inorg. Chem.* **2007**, *46*, 6933.
(37) Salvador, J. R.; Kanatzidis, M. G. *Inorg. Chem.* **2006**, *45*, 7091.
(38) Sebastian, C. P.; Kanatzidis, M. G. *J. Solid. State. Chem.* **2010**, *183*, 2077.
(39) Sebastian, C. P.; Malliakas, C. D.; Chondroudi, M.; Schellenberg, I.; Rayaprol, S.; Hoffmann, R. D.; Pottgen, R.; Kanatzidis, M. G. *Inorg. Chem.* **2010**, *49*, 9574.
(40) Sebastian, C. P.; Salvador, J.; Martin, J. B.; Kanatzidis, M. G. *Inorg. Chem.* **2010**, *49*, 10468.
(41) Subbarao, U.; Peter, S. C. *Inorg. Chem.* **2012**, *51*, 6326.

(42) Peter, S. C.; Kanatzidis, M. G. *Z. Anorg. Allg. Chem.* **2012**, *638*, 287.
(43) Subbarao, U.; Gutmann, M. J.; Peter., S. C. *Inorg. Chem.* **2013**, *52*, 2219.
(44) Subbarao, U.; Sebastian, A.; Rayaprol, S.; Yadav, C. S.; Svane, A.; Vaitheeswaran, G.; Peter, S. C. *Cryst. Growth Des.* **2012**, *13*, 352.
(45) Subbarao, U.; Peter, S. C. *Cryst. Growth Des.* **2013**, *13*, 953.
(46) Peter, S. C.; Sarkar, S.; Kanatzidis, M. G. *Inorg. Chem.* **2012**, *51*, 10793.
(47) Sarkar, S.; Peter, S. C. J. *Chem. Sci.* **2012**, *124*, 385.
(48) Gladyshevskii, E. I.; Bodak, O. I.; Yarovets, V. I.; Gorelenko, Y. K.; Skolozdra, R. V. *Ukr. Fiz. Zh.* **1978**, *23*, 77.
(49) Jutzi, P.; Schubert, U. *Silicon Chemistry*; Wiley VCH: Weinheim, 2007.
(50) Kittel, C. *Introduction to Solid State Physics*, 7th ed.; John Wiley & Sons: Hoboken, NJ, 1996.
(51) Buzea, C.; Robbie, K. *Supercond. Sci. Technol.* **2005**, *18*, R1.
(52) Andrzejewski, B.; Kowalczyk, A.; Frackowiak, J. E.; Tolinski, T.; Szlaferek, A.; Pal, S.; Simon, C. *Phys. Status Solidi B* **2006**, *243*, 295.
(53) Drulis, H.; Gaczynski, P.; Iwasieczko, W.; Suski, W.; Kotur, B. Y. *Solid State Commun.* **2002**, *123*, 391.
(54) Snyder, G. J.; Booth, C. H.; Bridges, F.; Hiskes, R.; DiCarolis, S.; Beasley, M. R.; Geballe, T. H. *Phys. Rev. B* **1997**, *55*, 6453.
(55) Hemberger, J.; Lobina, S.; von Nidda, H. A. K.; Tristan, N.; Ivanov, V. Y.; Mukhin, A. A.; Balbashov, A. M.; Loidl, A. *Phys. Rev. B* **2004**, 70.
(56) Quezel, S.; Tcheou, F.; Rossatmignod, J.; Quezel, G.; Roudaut, E. *Physica B+C* **1977**, *86*, 916.
(57) Cooke, A. H.; Martin, D. M.; Wells, M. R. *J. Phys. C: Solid State Phys.* **1974**, *7*, 3133.
(58) Gopal, E. S. R. *Specific Heat at Low Temperatures*; Plenum: New York, 1966.
(59) Falkowski, M.; Kowalczyk, A.; Tolinski, T. *J. Alloys Compd.* **2011**, *509*, 6135.
(60) Ragel, F. C.; du Plessis, P. D.; Strydom, A. M. *J. Phys.: Condens. Matter* **2009**, *21*, 046008.